

Modelling and Mitigating Multipath and NLOS for Cooperative Positioning in Urban Canyons

Joon Wayn Cheong, Eamonn Glennon, Andrew G. Dempster

Australian Center for Space Engineering Research
School of Electrical, Electronics and Telecommunications Engineering
University of New South Wales, Sydney 2052 Australia
Phone: +(61) 2 93856702
Email: cjwayn@unsw.edu.au

Damien Serant, Thibaud Calmettes

Thales Alenia Space, France
26 avenue J.F. Champollion
BP 33787
31037 Toulouse Cedex 1
Email: damien.serant@thalesaleniaspace.com

ABSTRACT

Existing investigations into integrating GNSS and Vehicle-to-Vehicle (V2V) ranging systems for Cooperative Positioning (CP) has evidenced its superiority in enhancing positioning accuracy. However, the ramifications of multipath – especially in terrestrial V2V measurements – have typically been neglected. This paper seek to effectively minimise the positioning error particularly in such circumstances using a modified particle filter technique.

The development of a scenario-based multi-sensor time-series simulator is described. The simulator simulates the multipath/NLOS errors for GPS and V2V measurements based on the location of the vehicles and GPS satellites and the interaction of GPS and V2V signals with a predefined virtual environment. The simulation is made even more realistic by using NetLogo to simulate each vehicle's motion. The INS measurement of each vehicle is also simulated based on the vehicle's motion. This software package thus provides a complete set of simulated measurements for V2V, GPS and INS. By adopting this method of simulating sensor outputs, arbitrary assumptions of multipath/NLOS simulation parameters can be avoided.

An estimation filter based on a modified particle filter that integrates GPS+V2V+INS sensors is implemented. This estimator is specifically designed to mitigate multipath/NLOS. Experiment result shows that the modified particle filter can still achieve Root Mean Squared Error (RMSE) of approximately 3m despite the presence of multipath/NLOS errors of up to 90m. In the same scenario, the generic particle filter produced RMSE of approximately 13m. In more extreme cases of NLOS, the generic particle filter has failed to produce valid estimates entirely whereas the modified

particle filter can still maintain a RMSE of approximately 3m.

KEYWORDS: Multipath, Non-Line-Of-Sight (NLOS), Cooperative Positioning, C-ITS

1. INTRODUCTION

Contrary to popular belief and television science fiction, satellite-based GNSS signals do not produce sub-meter accuracy position anywhere in the world. The high accuracies described in many existing literatures will only apply in clear sky conditions where line-of-sight (LOS) to at least four GNSS satellites is available. Navigation using GPS equipment in urban environment is highly susceptible to multipath and non-line-of-sight phenomenon due to large and smooth reflective building surfaces nearby and frequent obstruction of the line-of-sight signals between the user's equipment (UE) and the GPS satellite. Typical references to Real-Time Kinematic (RTK) equipments that are capable of delivering centimeter level accuracies fail in such urban environments because of the poor quality of the received GPS signals. A navigation system that purely relies on GPS will exhibit tens of meters of error in these GPS challenging scenarios, making even street level accuracies difficult to achieve and intermittent unavailability of navigation solution due to obstructed view of the sky. One possible method to overcome this includes augmenting GPS with Inertial Navigation Sensor (INS). However, military-grade INS equipments with good long term stability are several orders of magnitude more expensive. Augmenting GPS with cheap Microelectromechanical System (MEMS) INS can only partially alleviate the problem because it has extremely poor long-term stability.

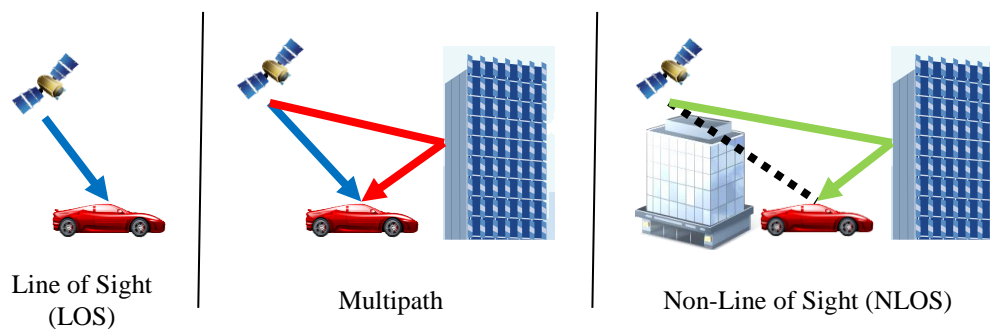


Figure 1 Illustration of the differences between Line of Sight (LOS – blue arrow), multipath (combination of blue arrow and red arrow) and Non-line of Sight (NLOS – green arrow) scenarios. Dotted black line indicates obstructed LOS.

Line of Sight (LOS) is the case where the signal path between the transmitter (i.e. GPS satellite) and the receiver is unobstructed and does not contain other signal components due to interaction of the signal and its environment. This is the best case scenario for ranging and positioning purposes. Multipath is a phenomenon where the received signal contains the LOS signal summed with one or more delayed version of the signal that has been reflected off its physical surrounding. Non-Line of Sight (NLOS) is the worst case scenario where the LOS component is entirely obstructed but the transmitter's signal can still be detected by the receiver via reflections off its physical surroundings.

Multipaths in GPS measurements are inevitable, especially in urban environments. Multipath mitigation technologies exists in the correlator (i.e. signal processing) level but can only be limited and cannot be entirely eliminated. Multipath components of tens of meters will still be

present. As an example, a commercial grade Ashtech DG14 GPS receiver released in 2013 still cannot mitigate multipath components smaller than 37 meters. On the other hand, adding this functionality to the correlator will incur losses in signal detection sensitivity. This is a known trade-off (Mubarak 2010). Also, most of these techniques only work when the line-of-sight signal is stronger than the multipath. If this is not true, the techniques amplify the multipath error. To realise lower multipath errors would yield a significantly lower SNR that would hamper the ability of the GPS receiver to receive the least 3/4 GPS signals necessary for 2D/3D positioning. As GPS receiver manufacturers opt for higher sensitivity to maximize positioning availability, multipath mitigation capabilities are typically limited or non-existent. Even if multipath can be entirely mitigated, NLOS - which are predominant in urban environments – still cannot be avoided, and NLOS cannot be distinguished at the correlator level. Hence, robustness against NLOS has to be implemented in the navigation processing level due to the inability of the correlator to distinguish between LOS and NLOS signal.

2. COOPERATIVE INTELLIGENT TRANSPORT SYSTEMS

In Cooperative Intelligent Transport Systems (C-ITS), participating vehicles are fitted with Dedicated Short Range Communication (DSRC) equipment to allow communication of crucial data such as each vehicle's estimated position and speed between vehicles for safety applications. It has been proposed that inter-vehicular communication systems are capable of obtaining Vehicle-to-vehicle (V2V) range measurements via some form of Time of Arrival (TOA) radio ranging. (Alam and Dempster 2013; Efatmaneshnik et al. 2012)

The concept of C-ITS and the development of DSRC are based on the core assumption that each vehicle has a sufficiently accurate knowledge of its own position. However, this assumption will prove to be flawed when the vehicle is navigating in deep urban environment. At road intersections where the vehicle is surrounded by obstructions such as sky-scrapers, collision may be unavoidable by the time when two vehicles come within field-of-vision of each other. Note that anti-collision systems that rely on radar, laser or optical technologies require the potential threat to be within field-of-vision to produce any useful indication. As a consequence, the current state of technology will be unable to alert drivers to visually unobservable oncoming traffic in GPS-challenged environments. This jeopardises the safety-critical application of C-ITS, which is to provide warning to impending vehicle-to-vehicle collision.

This paper proposes a system that integrates all three types of sensors, GPS, V2V and Inertial Navigation Sensor (INS) measurements/observations into the position-domain filter. In contrast to single-epoch robust estimation algorithms, the concepts presented in this paper demonstrates the further improvements that can be obtained using a robust multiple epoch position-domain filtering. This type of filtering can be conventionally achieved via an Extended Kalman Filter (EKF) when robustness is not considered. But EKF is derived from the non-robust LS estimator that operates on linearised Gaussian system of equations. The robust estimator proposed herein is piecewise defined, which mathematically renders the EKF inapplicable. Hence, a new method of processing position-domain filtering based on the robust estimator is necessary. A viable method that this paper explores to achieve this goal is the particle filter.

3. SCENARIO-BASED SENSOR SIMULATOR

To validate the proposed integrated system, a simulation for a realistic multipath and NLOS

environment is necessary. Simulating the sensor outputs via random processes is often unjustifiable. This is because the probability of occurrence of NLOS and multipath vary from time to time as its physical surrounding changes over time. The probability of NLOS/multipath occurrence is not entirely random either as this probability maintains its value for a particular physical environment. Hence, this paper undertakes a scenario-based approach to simulate perturbations in the measured V2V ranges and GPS pseudoranges due to multipath and NLOS. As a result, it is not necessary for the scenario-based simulator to assume probabilities of NLOS or probabilities of multipath that are often arbitrary.

The scenario simulates a target vehicle travelling in the east direction from circa East -1500m (where there are no buildings) into an urban environment where tall buildings are concentrated within $\pm 800\text{m}$ East and $\pm 400\text{m}$ North. The heights of the buildings vary from 50m to 150m with a median of circa 70m. This choice of building heights is typical of an urban city such as Sydney. A snapshot of this simulated environment which consists of 9 buildings is shown in Figure 2.

The simulation of vehicle motion and interaction are based on NetLogo (Tisue and Wilensky 2004) whereby vehicles brake and accelerate according to traffic conditions. In all four cases a target vehicle travelled a similar path of about 2 km. The target traffic density simulated is 600 vehicles per hour. The simulation duration depended on the traffic conditions which in this case is 462 seconds. The coverage of V2V signals are set at 250 m, similar to DSRC specifications. Note that all coordinates referred to in this paper follows the East-North-Up coordinate system.

The changes in the simulated environment with respect to the target vehicles varies the simulation parameters for its sensors and impose sky view restrictions on GPS pseudorange measurements makes the simulation more realistic. These elaborate simulations also account for obstructions between vehicles (e.g. buildings) that prohibit V2V measurements to be observed.

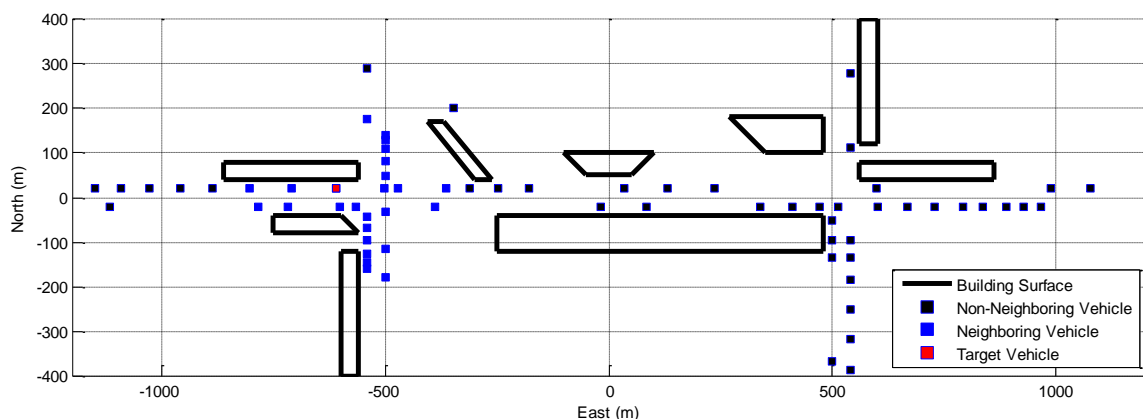


Figure 2 Urban scenario and traffic model to dictate the presence/absence and magnitude of multipath/NLOS

3.1 GPS Simulator: Multipath and NLOS

As introduced previously, the effect on ranging error for multipath and NLOS cases are different. The GPS measurement simulator has been implemented to model such differences. Multipath error or multipath delay is defined as the relative time delay between the LOS

signal component and the delayed signal component via the reflection path. In the case of multipath, the LOS signal component interacts with the multipath signal component in the correlator to produce a ranging error (i.e. measurement error) that has an indirect relationship with the multipath delay. Figure 3 is produced by the multipath model implemented and is verified to be commensurate with existing literatures (Kaplan and Hegarty 2006).

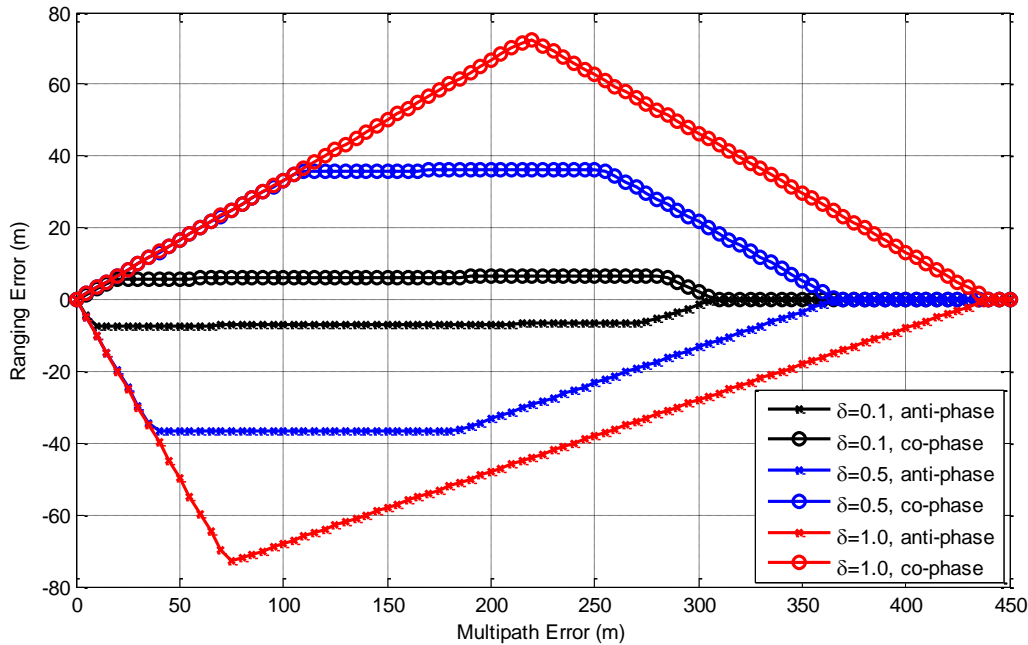


Figure 3 Multipath Error Envelope for relative amplitude $A=0.5$ at various code correlator spacing δ

Several other parameters affect the multipath-induced ranging error. These include the code correlator's Early-Late spacing δ , the relative carrier phase between the LOS signal component and the multipath signal component, and the relative amplitude A between the LOS signal component and the multipath signal component. Figure 3 shows the upper and lower limits for the ranging error for a given δ and A which forms the ranging error envelope. Depending on its relative carrier phase, the ranging error can be any value on or between the limits.

However, the ranging error due to NLOS is modeled directly as the multipath delay. Hence, unlike multipath, the error due to NLOS is unlimited and can be as large as its interaction with the physical environment dictates.

The scenario-based GPS measurement simulator evaluates the obstruction and reflection due to buildings along and around the signal path, respectively. This computation is a two step process. The transmitted GPS signal is modeled as rays interacting with the unit normal vector of each surface which then allows the algorithm to determine if the surface is an obstruction or a reflector. Then, the validity of the obstruction or reflection is determined. The multipath error model is used if the LOS path is unobstructed and a reflection is present. The NLOS error model is used if the LOS path is obstructed but a reflection is present. The simulator also identifies cases where measurements are unobservable due to obstructions.

In Figure 4, the simulation is paused at 329 seconds to verify the ability of the simulator to classify LOS, NLOS and multipath cases for GPS measurements. By implementing a plotting script that plots each signal component, the validity of each obstruction and reflection can be visually verified.

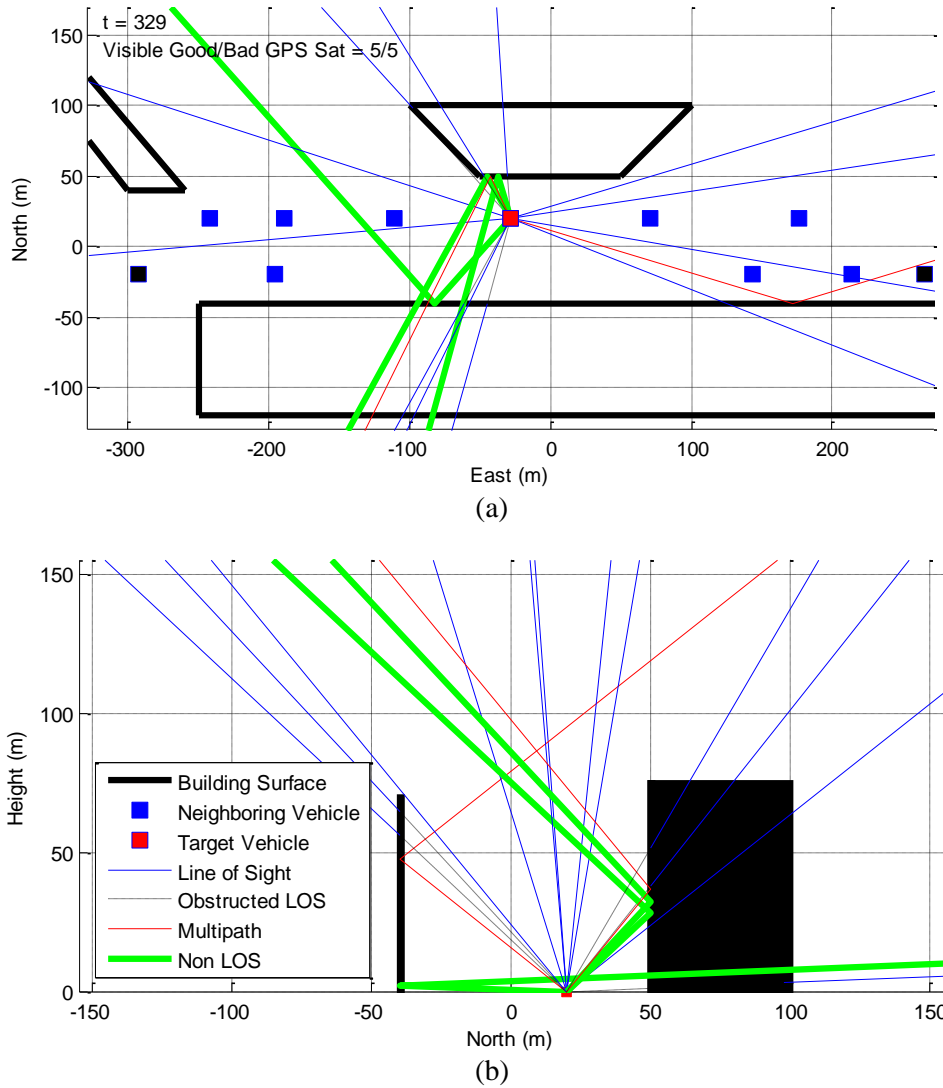


Figure 4 Signal paths of the GPS signals received by the target vehicle and its interaction with its environment. (a) Top View, (b) Side View.

3.2 V2V Simulator: Multipath and NLOS

The implementation for the V2V measurement simulator is similar to the simulator for GPS. This is true except that the calculation of the incident ray on the each surface has to be recomputed differently. The effect of multipath is modeled based on a signal with 10MHz bandwidth, which translates to 30m in range. Thus, it is assumed that multipath components beyond 30m is distinguishable and can be eliminated.

In Figure 5, the scenario is paused at epoch 220 seconds to illustrate the simulated interaction of signals with buildings due to NLOS, multipath and obstruction. The validity of reflections can be verified by observing that the angle of incidence is always equal to the angle of reflection.

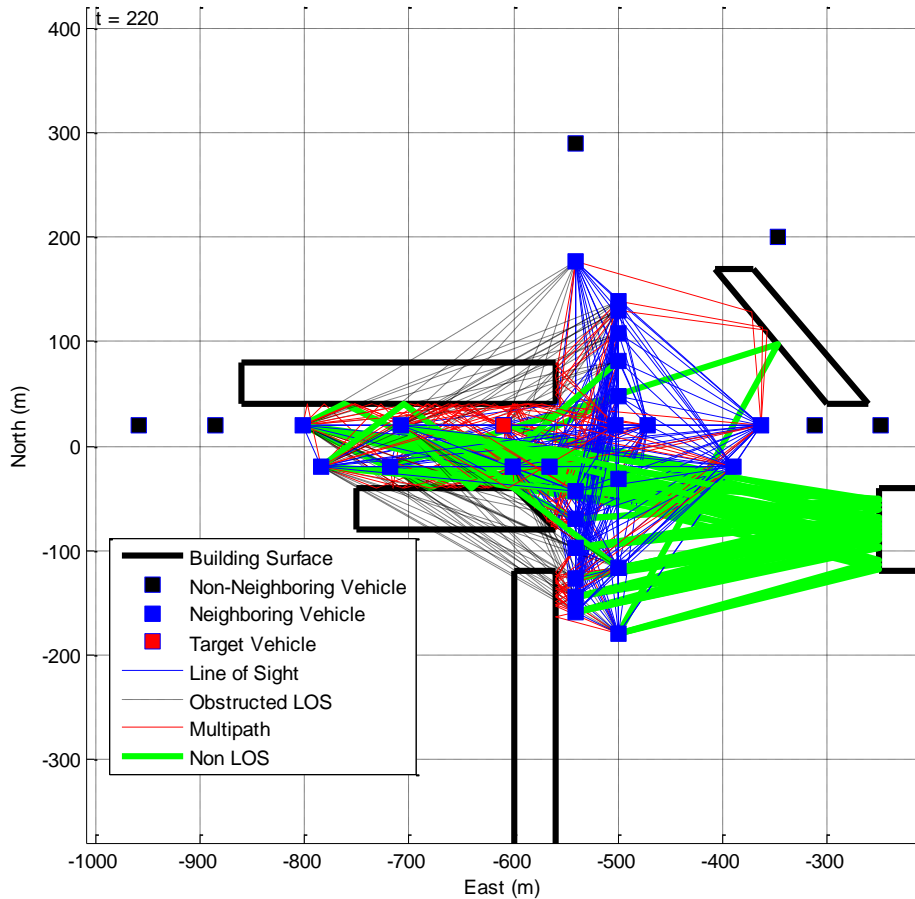


Figure 5 Illustration of the simulated interaction of signals with buildings due to NLOS, multipath and obstruction.

3.3 Gyroscope and Accelerometer Simulator

This section describes the implemented simulator for a 6-axis Inertial Measurement Unit (IMU) which comprises of a 3-axis gyroscope and a 3-axis accelerometer. The simulator emulates the signal dynamics component due to vehicle motion and the noise component inherent in MEMS INS technologies. The motion-dependant signal dynamics is simulated and implemented but is not described here for brevity. The sensor noise parameters in this simulator are taken from the datasheet of the X-Sense MT-100 IMU. The Allan deviation of this device has been evaluated by Thales Alenia Space and shown in Figure 6. The selected points in the Allan deviation plot is used as noise parameters as described in (Woodman 2007).

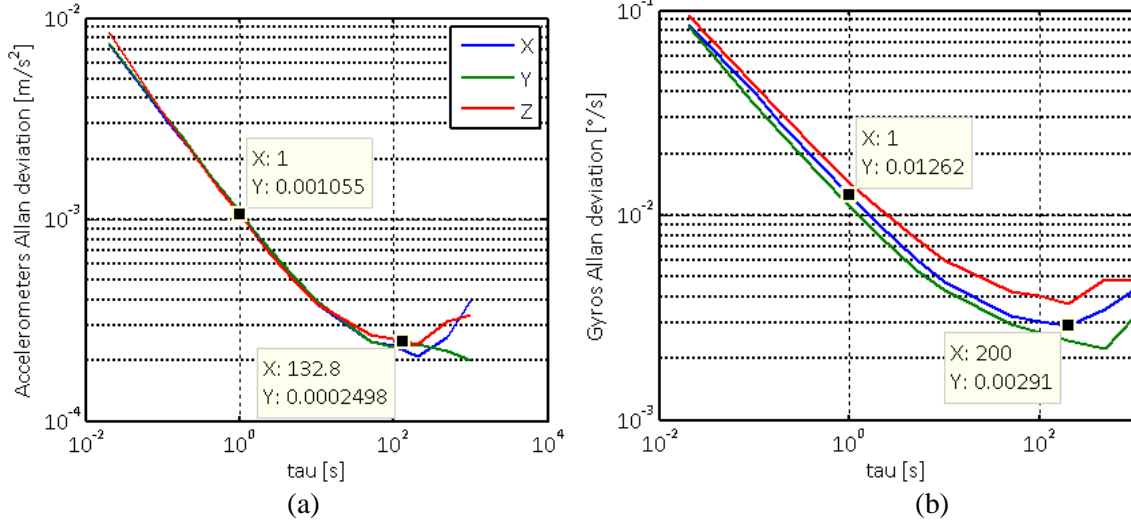


Figure 6 X-Sens MT-100 (a) Accelerometer and (b) Gyroscope Allan Deviation

Bias Stability is obtained at the minimum of the flattening of the Allan Curve while the noise density is obtained at $\tau=1s$. Given that δt is the sampling period in seconds (implemented for 1 second), and t is the time (in seconds) at the minimum of the flattening of the Allan Curve. The errors in gyroscope are simulated as:

$$e_i = m_i + \sum_i N_i + \dot{\varphi}_i$$

where $N_i \sim N(0, \sigma_b)$ is the normally distributed variable with STD of σ_b , $\dot{\varphi}_i \sim N(0, \sigma_n)$ and m_i is the true sensor output in zero-noise. σ_b is defined as $\sigma_b = BI / \sqrt{\delta t}$ and σ_n is defined as

$$\sigma_n = \sqrt{\delta t / t}$$

Table 1 Bias Instability and Noise Density figures implied by the Allan curve

	Bias Instability, BI	Noise Density, ND
Gyroscope	0.00291 °/s @ $\tau=200s$	0.01262 °/s/ \sqrt{s}
Accelerometer	0.00025 m/s ² @ $\tau=133s$	0.001055 m/s ² / \sqrt{s}

In addition to simulating these measurements, an independent module is implemented to verify the INS measurements by estimating the navigation solution from the simulated sensor measurements in zero-error condition. The INS-based navigation algorithm is implemented based on (Woodman 2007). The simulated measurements have been demonstrated to pass the verification test.

Figure 7 show an example of the generated sensor measurements embedded in noise based on the target vehicle in the scenario previously described.

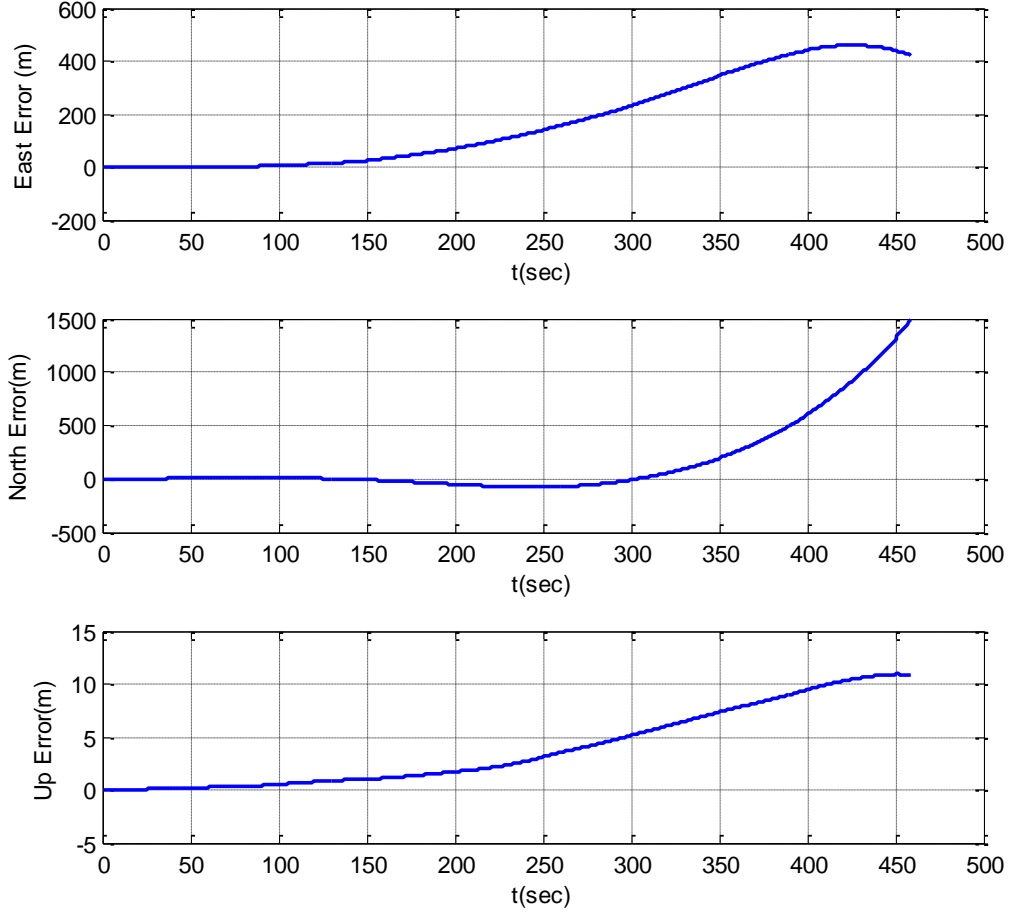


Figure 7 Positioning Error in local ENU coordinates using INS-only sensors.

4. MODIFIED PARTICLE FILTER FOR MULTIPATH MITIGATION

The rest of this work attempts to investigate the positioning performance of Particle Filter (PF) for GPS/V2V/INS integration in realistic urban scenarios using the simulator modules described previously. A method that is capable of mitigating measurement outliers due to multipath/NLOS is also proposed. A case study of the performance of the generic PF is compared against the modified PF.

At time instant t , let v_t denote the vehicle position (i.e. state), z_t be the vector of observation for V2V range, GPS pseudorange and INS measurements. In the particle filter implementation, N_t particles that contain the state and weight information $\{v_t^i, w_t^i\}_{i=1}^{N_t}$ is instantiated. The implementation of the particle filter herein follows the Generic Particle Filter algorithm as described in (Arulampalam et al. 2002). For completeness, this algorithm is summarized as following:

Algorithm 1 Generic Particle Filter

Initialise: Sample $\{v_o^i\}_{i=1}^{N_t}$ from $p(v_o)$, set $w_o^i = 1/N_t$ for $\forall i$

for each time instant t

Sample v_t^i from $p(v_t | v_{t-1}^i, z_k)$

<p>Calculate weights for each particle $w_t^i = w_{t-1}^i \cdot p(z_t v_t^i)$</p> <p>Normalise weights for each particle $w_t^i \leftarrow \frac{w_t^i}{\sum_i w_t^i}$</p> <p>Output state estimates: $\hat{v}_t = \sum_i w_t^i v_t^i$</p> <p>Resample the particles $\{v_t^i, w_t^i\}_{i=1}^{N_t}$</p> <p>end</p>

A generic Particle Filter (PF) dictates that the observation-based probability $p(z_t | v_t^i)$ should be evaluated as:

$$p(z_t | v_t^i) = p(z_t^{INS} | v_t^i) \prod_k p(z_t^{GPS}(k) | v_t^i) \prod_l p(z_t^{V2V}(l) | v_t^i)$$

The probabilities follow the normal distribution while the STD of the normal distribution is different for each type of measurement. In this implementation, the STD for GPS pseudorange measurements is defined as 3m, which is justified in Alam (2012). The STD for INS measurement is arbitrarily chosen as 1m/s². The V2V measurements' STD for $p(z_t^{V2V}(l) | v_t^i)$ is chosen as 15m despite that the simulated V2V measurement noise STD is significantly smaller. This is because multipath is consistently present in the simulated urban environment (as can be observed in Figure 5) which is effectively equivalent to an enlarged STD.

Now, consider that some of the GPS and V2V observations are outliers due to multipath and NLOS. One notable fact would be a lower peak in the joint PDF $p(z_t | v_t^i)$. In extreme cases where NLOS is in the order of a hundred meters, $p(z_t | v_t^i)$ may asymptotically evaluate to zero due to one or more extreme outlier. This effect can be observed in the performance evaluation subsection later. More importantly however, is that the peak of the joint PDF in the state space will shift due to this outlier which will produce large localization errors as a result. To illustrate this effect, time instant 329 (refer to Figure 4) is identified as a crucial time segment to evaluate the robustness of algorithms against outliers in the GPS measurement domain. Here, five LOS and five multipath/NLOS signals are present. Figure 8 illustrates the PDF of individual GPS pseudorange measurements and its resulting joint PDF. By using a generic PF, it is shown that the peak of its joint PDF is approximately 30m away from the true position. Note that the difference in amplitudes in Figure 8 is illustrated to allow better visualization and does not signify any difference in likelihood or probability.

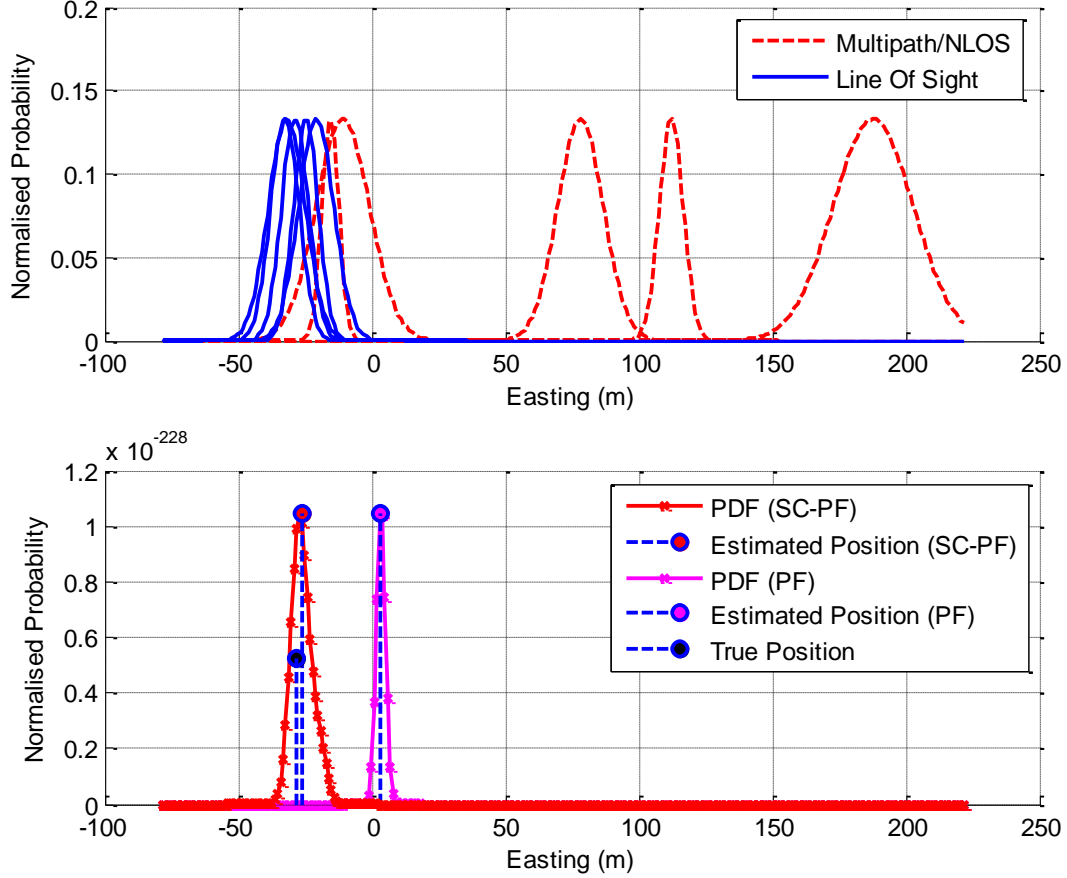


Figure 8 Normalised PDF of each GPS measurement (top) and the joint PDF and estimated positions of respective algorithms (bottom)

To circumvent the effect of outliers, it is important to understand that not all measurements need to be accounted for in the joint PDF. As explained in well-established GPS textbooks (Kaplan and Hegarty 2006), generally four GPS LOS observations are sufficient to produce valid positioning. However, more measurements can attribute to higher positioning accuracy provided that the additional measurements are also LOS. Hence, choosing the subset of GPS measurements that are outlier-free will produce a position solution that is closer to the true position. Another feature that can be identified from Figure 8 is that the PDF of outlying GPS measurements are largely non-intersecting in the position space whereas the PDF of LOS measurements are all intersecting around the true position. Hence, the peak of the joint PDF of a measurement subset that contains outliers will be consistently lower than its outlier-free counterpart.

Exploiting the two core features of the joint PDF, it is proposed in this paper that each particle sees a different subset of the measurement where the size of the subset is a random integer between 4 and the total number of observed measurements. The selection of measurements to be combined is also randomly determined. This method is referred to as Selective Combining Particle Filter (SC-PF). Hence, given a random subset of measurement for the i -th particle for GPS measurements Γ_t^i and V2V measurements Ξ_t^i , the joint PDF in the modified implementation is given by,

$$p(z_t | v_t^i) = p(z_t^{INS} | v_t^i) \prod_{k \in \Gamma_t^i} p(z_t^{GPS}(k) | v_t^i) \prod_{l \in \Xi_t^i} p(z_t^{V2V}(l) | v_t^i)$$

Note that the core difference between PF and SC-PF is in their definition of probability of observation given a particle's state. The joint PDF for the SC-PF assuming infinitely many particles is shown in Figure 8. In this plot, it is evidently shown in this scenario that the joint PDF for SC-PF is a better estimate than PF.

The scenario-based simulators described in earlier sections are employed to provide all three types of measurements for a realistic time-series evaluation of outlier mitigation performance of the described navigation algorithms in urban environments. One method of evaluating the tolerance of an algorithm against outliers is by observing its implied residuals. Given an estimated position, it is possible to evaluate the pseudoranges or ranges implied by the estimated position. The difference between the measured pseudoranges or ranges and its position-implied counterpart is thus referred to as the position-implied residual. Figure 9 shows the GPS residuals implied by the positions estimated by SC-PF. The degree of similarity between this and the true residuals is a clear evidence of the ability of SC-PF to tolerate outliers and not over-fit the estimated position to outliers.

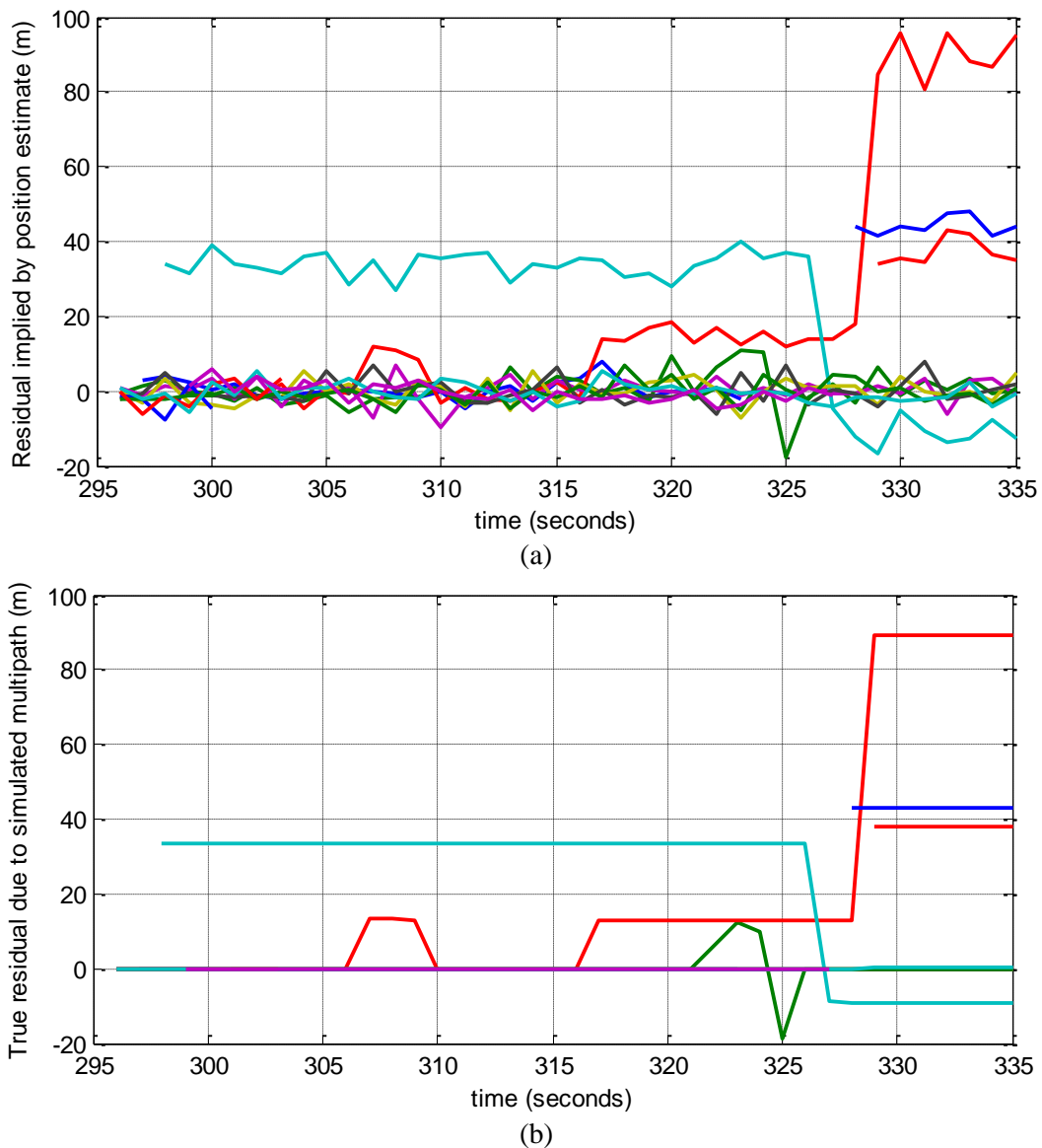


Figure 9 (a) GPS measurement residual implied by the estimated position by SC-PF and (b) true residuals. Different colours correspond to different measurements.

Paying a closer attention to the difference between the position-implied GPS residuals and the true GPS residuals, this difference is evaluated for both SC-PF and PF algorithms in Figure 10. This figure clearly shows that SC-PF is able to produce position-implied residuals that closely match the true residuals expected from simulated multipath. As a result, SC-PF exhibits lower error magnitude than PF in Figure 11.

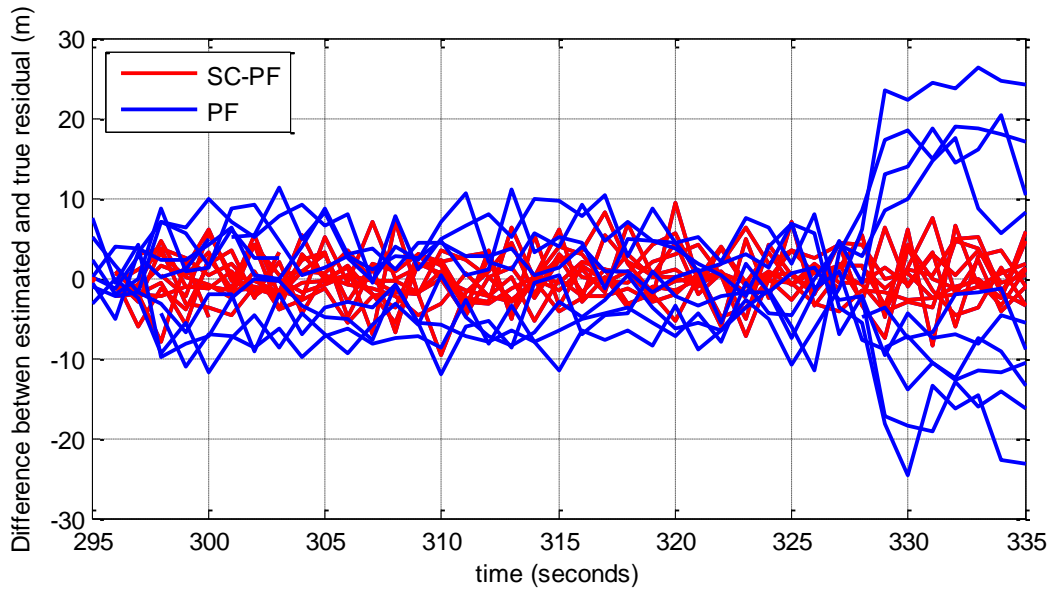
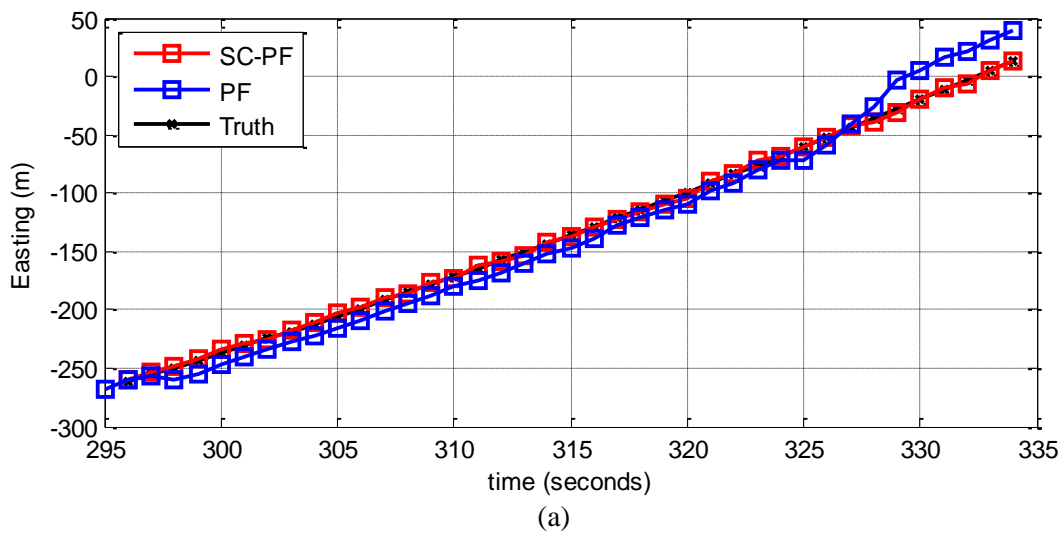


Figure 10 Difference between the position-implied GPS residuals and the true GPS residuals



(a)

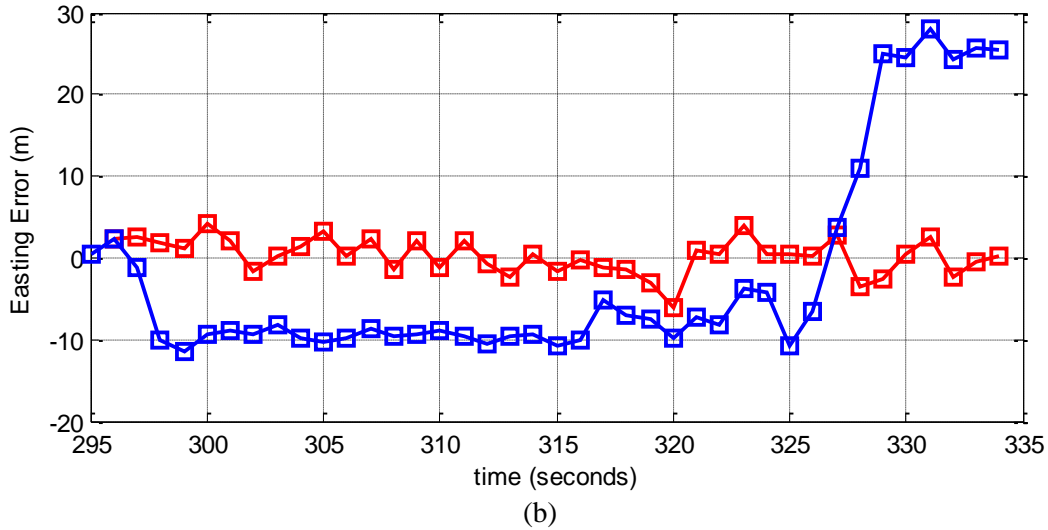


Figure 11 Estimated and true (a) easting position and (b) easting error for both algorithms.

Figure 11 shows the estimated position based on SC-PF and PF and its corresponding error. Note that the both subfigures follow the same plot legend. By cross referencing the results in this figure with Figure 9(b), it can be observed that the positioning error for SC-PF is considerably smaller than PF especially in the presence of simulated multipath/NLOS which is evident after the first few epochs. Both algorithms exhibit smaller errors in the first few epochs due to the absence of significant multipath/NLOS. The RMSE in this time segment ($t = 295 - 335s$) for both algorithms are presented in Table 2. In the PF implementation that involves GPS measurement, its RMSE is around five times larger than SC-PF. This result is unsurprising as Figure 11(b) clearly corroborates this observation. By and large, the RMSE for V2V+INS integration in this time segment shows that the performance of SC-PF and PF is similar.

Recall that the PF effectively falls apart when multipath/NLOS errors are excessive because the weights of all particles will evaluate to zero, hence producing an invalid result. This effect has been identified for PF in a particular time segment ($t = 199 - 224s$) due to extreme outliers in V2V measurements. The simulated physical environment for this time segment has been illustrated in Figure 5. As can be seen in Table 2, the SC-PF still continue to produce nominal RMSE levels despite the presence of large outliers in V2V measurements.

Due to various time segments where PF is unable to produce valid positions, the results for the full duration of the simulation are unable to be produced for an overall comparison.

Table 2 Root Mean Square Error (RMSE) of SC-PF and PF in GPS-challenged environment ($t = 295 - 335s$) and V2V-challenged environment ($t = 199 - 224s$)

	$t = 295 - 335s$		$t = 199 - 224s$	
	SC-PF	PF	SC-PF	PF
GPS+INS	2.7 m	13.9 m	2.0 m	4.6 m
V2V+INS	2.2 m	2.4 m	2.7 m	N/A
GPS+V2V+INS	2.2 m	12.7 m	2.8 m	N/A

5. CONCLUSION

The paper has achieved two major goals. The first is that a scenario-based simulation platform for GPS, V2V and INS sensors has been developed and verified. The simulator accounts for signal perturbations including noise, multipath, NLOS and obstructions given a target vehicle's position and its physical environment. Using the scenario-based simulator, the second and more important outcome shows that a GPS+V2V+INS integrated particle filter is capable of mitigating multipath and NLOS. Experiment result shows that the modified particle filter can still achieve RMSE of approximately 3m despite the presence of multipath/NLOS errors of up to 90m. In the same scenario, the conventional particle filter produced RMSE of approximately 13m. In more extreme cases of NLOS, the conventional particle filter has failed to produce valid estimates entirely whereas the modified particle filter can still maintain a RMSE of approximately 3m.

REFERENCES

- Alam, N., and A. G. Dempster. 2013. "Cooperative Positioning for Vehicular Networks: Facts and Future." *Intelligent Transportation Systems, IEEE Transactions on* 14 (4):1708-17. doi: 10.1109/tits.2013.2266339.
- Alam, Nima. 2012. "Vehicular positioning enhancement using DSRC." PhD Thesis, University of New South Wales.
- Arulampalam, M Sanjeev, Simon Maskell, Neil Gordon, and Tim Clapp. 2002. "A tutorial on particle filters for online nonlinear/non-Gaussian Bayesian tracking." *Signal Processing, IEEE Transactions on* 50 (2):174-88.
- Efatmaneshnik, Mahmoud, Nima Alam, Allison Kealy, and Andrew G Dempster. 2012. "A Fast Multidimensional Scaling Filter for Vehicular Cooperative Positioning." *The Journal of Navigation* 65 (02):223-43. doi: doi:10.1017/S0373463311000610.
- Kaplan, ED, and CJ Hegarty. 2006. *Understanding GPS: Principles and applications*: Artech House.
- Mubarak, Omer Mohsin. 2010. "Multipath mitigation for GPS signals exploiting carrier phase." PhD Thesis, University of New South Wales.
- Tissue, Seth, and Uri Wilensky. 2004. Netlogo: A simple environment for modeling complexity. Paper presented at the International Conference on Complex Systems.
- Woodman, Oliver J. 2007. "An introduction to inertial navigation." *University of Cambridge, Computer Laboratory, Tech. Rep. UCAMCL-TR-696* 14:15.